



ELSEVIER

Earth and Planetary Science Letters 198 (2002) 307–322

EPSL

www.elsevier.com/locate/epsl

# Re–Os evidence for replacement of ancient mantle lithosphere beneath the North China craton

Shan Gao<sup>a,b</sup>, Roberta L. Rudnick<sup>c,\*</sup>, Richard W. Carlson<sup>d</sup>,  
William F. McDonough<sup>c,1</sup>, Yong-Sheng Liu<sup>b</sup>

<sup>a</sup> Key Laboratory of Continental Dynamics, Department of Geology, Northwest University, Xi'an 710069, PR China

<sup>b</sup> Faculty of Earth Sciences, China University of Geosciences, Wuhan 430074, PR China

<sup>c</sup> Department of Earth and Planetary Sciences, Harvard University, Cambridge, MA 02138, USA

<sup>d</sup> Department of Terrestrial Magnetism, Carnegie Institution of Washington, 5241 Broad Branch Road, N.W., Washington, DC 20015, USA

Received 25 July 2001; received in revised form 7 January 2002; accepted 23 January 2002

## Abstract

Re–Os data for peridotite xenoliths carried in Paleozoic kimberlites and Tertiary alkali basalts confirm previous suggestions that the refractory and chemically buoyant lithospheric keel present beneath the eastern block of the North China craton (and sampled by Paleozoic kimberlites) is indeed Archean in age and was replaced by more fertile lithospheric mantle sometime after the Paleozoic. Moreover, lithospheric mantle beneath the central portion of the craton (west of the major gravity lineament) formed during the last major Precambrian orogeny, around 1900 Ma ago. This age is significantly younger than the overlying crust (2700 Ma), suggesting that the original Archean lithosphere was replaced in the Proterozoic. The timing of lithospheric replacement in the eastern block of the North China Craton is constrained only to the Phanerozoic by the Re–Os results. Circumstantial geologic evidence suggests this new lithosphere is Jurassic or Cretaceous in age and formed after collision of the Yangtze and North China cratons in the Triassic, an event that was also responsible for the subduction and uplift of ultrahigh-pressure metamorphic rocks. Collectively, these data suggest that lithosphere replacement occurred in response to two continent collisional events widely separated in time ( $\sim 1900$  and  $\sim 220$  Ma). Coupled with observations from other Archean cratons we suggest that wholesale replacement of lithospheric mantle ( $\pm$  lower crust) may require large-scale continental collision. © 2002 Elsevier Science B.V. All rights reserved.

**Keywords:** Re/Os; isotope ratios; Archean; Mantle; North China Platform; delamination

## 1. Introduction

Cratons are ancient continental regions that have been tectonically quiescent for billions of years. They are characterized by low surface heat flow (average = 40 mW/m<sup>2</sup> [1,2]) and are underlain by mantle that is seismically fast to depths on the order of 250–300 km [3,4]. These

\* Corresponding author. Present address: Geochemistry Laboratory, Department of Geology, University of Maryland, College Park, MD 20742, USA. Fax: +1-301-314-9661.

E-mail address: rudnick@geol.umd.edu (R.L. Rudnick).

<sup>1</sup> Present address as corresponding author.

observations, coupled with the presence of cold, refractory mantle xenoliths carried in kimberlite pipes that erupt through cratons (e.g., [5]), have led to the hypothesis that Archean cratons are stabilized by the presence of cold, viscous, chemically buoyant lithospheric mantle keels that have inhibited tectonic disruption of the craton as it drifts across the Earth's surface [3,6].

The presence of a strong lithospheric keel beneath cratons has important implications for their strength, and possibly their stability (i.e., resistance to recycling). The presence of a thick and strong mantle keel inhibits material transfer from crust to convecting mantle via deep-seated processes such as foundering of dense, mafic lower crust (generally referred to as 'delamination' within the geochemical community, e.g., [7]). If the keels are absent, either because they never developed, or because they have been removed, cratons may experience magmatism and deformation, which may allow for lower crustal delamination and ultimately lead to continental break-up and recycling into the mantle.

Although most Archean regions are characterized by the presence of these keels, some are not. Peridotite xenoliths from the Mojavia terrane in the southern Basin and Range are much more Fe-rich than typical cratonic lithosphere, but formed at the same time as the overlying crust, in the late Archean/earliest Proterozoic [8]. Thus, although the Mojave block formed in the Archean, it did not develop a thick, insulating lithosphere and has consequently been strongly deformed during multiple orogenic events. In other Archean regions, the keel appears to have been removed to varying degrees. The Wyoming craton, for example, is lacking fast seismic wave speeds at depth [9,10], and xenolith studies have suggested that the Archean lithospheric mantle was strongly affected during Proterozoic mobile belt accretion [11] and was removed below 150 km, possibly during the Mesozoic Laramide orogeny [12].

The North China craton (Fig. 1) is one of the world's oldest Archean cratons, preserving crustal remnants as old as 3800 Ma [13]. The eastern part of the North China craton is perhaps the best example of an Archean craton that appears to have lost its lithospheric keel [14,15]. The lines

of evidence are well summarized in Griffin et al. [15] and include high surface heat flow, uplift and later basin development, slow seismic wave speeds in the upper mantle, and a change in the character of mantle xenoliths sampled by Paleozoic to Cenozoic magmas. Collectively, these observations have been used to suggest that ancient, cratonic mantle lithosphere, similar to that presently beneath the Kaapvaal, Siberian and other Archean cratons, was removed from the base of the eastern block of the North China craton sometime after the Ordovician, and replaced by younger, less refractory lithospheric mantle. Several issues remain uncertain:

1. Was all of the ancient lithosphere removed, or do remnants remain in restricted geographic locales?
2. What are the processes responsible for removal and replacement? and
3. When did these processes occur?

Menzies et al. [14] suggest that remnants of the ancient lithosphere may survive as harzburgites, and that removal was caused by indentor tectonics resulting from the collision of India and Eurasia, about 40 Ma ago. Griffin et al. [15] suggest that relict ancient lithosphere may persist in areas of thicker lithosphere, and may be underlain by more fertile Phanerozoic lithosphere. They suggest that removal may have been associated with Mesozoic and Cenozoic subduction and later rifting or the Triassic collision between the North China block and Yangtze craton. Zheng et al. [16] suggest that the present lithosphere is a mixture of ancient and newly accreted material and that lithospheric replacement is intimately associated with the Tan-Lu fault, a major strike-slip fault that crosscuts the eastern block of the North China craton.

In this paper we present Re–Os isotopic data for mantle samples from four xenolith localities within the North China craton that span eruption ages from Paleozoic to Cenozoic and areal distribution from the Trans-North China Orogen to the easternmost craton in the Shandong Peninsula. These data place constraints on the age of the lithosphere sampled in space and time and confirm previous suggestions that a profound change in the nature of the deep lithosphere occurred

between 400 Ma and 40 Ma (age of the host magmas) in the eastern block. Our data also provide evidence that a similar, but much more ancient, lithospheric change accompanied the formation of the Trans-North China Orogen around 1900 Ma. We use these results, coupled with regional geological evidence, to speculate on the causes of these changes.

## 2. Geologic background

Based on age, lithological assemblage, tectonic evolution and  $P$ – $T$ – $t$  paths, the North China Craton can be divided into the Eastern Block, the Western Block and the intervening Trans-North China Orogen/Central Orogenic Belt (Fig. 1) [17–20].

The basement of the Eastern Block consists primarily of Early to Late Archean high- and low-grade tonalitic, trondhjemitic and granodioritic (TTG) gneisses and 2500 Ma syntectonic granitoids, with rafts of Early to Late Archean

(3800–3000 Ma) granitic gneisses and supracrustal rocks, including ultramafic to felsic volcanic rocks and metasediments [17,18].

The Western Block is characterized by late Archean to Paleoproterozoic metasedimentary belts that unconformably overlie Archean basement [17,21,22], which consists of granulite facies TTG gneiss and charnockite (3300 Ma) [23] with minor mafic granulite and amphibolites.

Separating the two blocks is the Trans-North China Orogen, which extends as a roughly north–south trending belt across the North China Craton (Fig. 1). The orogen includes a series of 2500–2700 Ma amphibolite to granulite facies terrains (e.g., Huai'an, Fuping, Hengshan and Taihua) [17,18,24,25] and 2500 Ma greenschist facies granite–greenstone terrains (e.g., Wutai and Dengfeng) [17,18,24,25]. These are overlain by 2200–2400 Ma Paleoproterozoic sequences characterized by bimodal mafic and felsic volcanic rocks in the southern part of the orogen, and by thick carbonate and clastic sedimentary rocks interleaved with thin basalt flows in the central part of the orogen. These volcanosedimentary assemblages are characteristic of continental rifts [26].

There are contrasting views regarding the timing of the collision between the Western and Eastern Blocks, which formed the Trans-North China Orogen. Multi-grain zircon populations from TTG gneisses of the Trans-North China Orogen have upper intercept U–Pb ages of 2500–2700 Ma and lower intercepts of 1800–2000 Ma. These younger ages correspond to Sm–Nd ages of garnets from the high-pressure granulites and  $^{40}\text{Ar}/^{39}\text{Ar}$  ages of hornblendes in amphibolites and biotites in TTG gneisses, as well as SHRIMP zircon rim ages of the TTG gneisses and supracrustal rocks [17,18]. They are interpreted as the age of metamorphic overgrowth. These, together with near-isothermal decompressional clockwise  $P$ – $T$  paths, led Zhao et al. [17,18] to suggest collision occurred between the Eastern and Western Blocks at ca. 1800 Ma. However, a recent finding of a 2505 Ma ophiolite complex in the northern Trans-North China Orogen [19] implies a much older collisional event between the Western and Eastern Blocks. Li et al. [20,22] proposed a scenario that accommodates all these observations and assumes

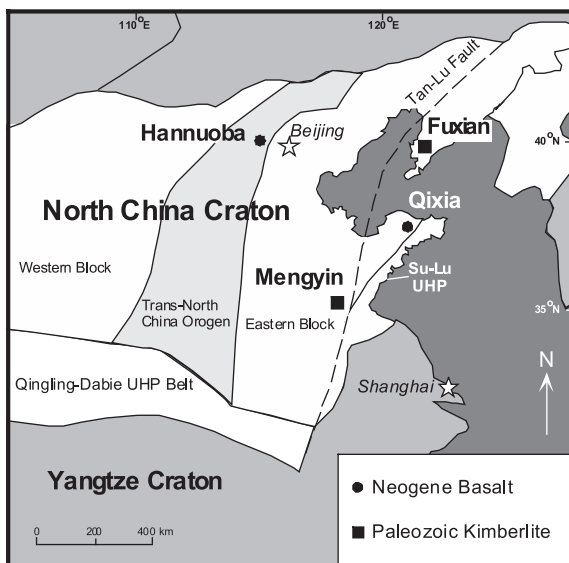


Fig. 1. Map showing xenolith localities referenced in the text relative to main geologic features of the North China craton. The Hannuoba locality lies within the Trans-North China Orogen, whereas Qixia, Fuxian and Mengyin all lie within the Eastern Block of the North China craton. Star represents capital city.

collision occurred between the two blocks at 2500 Ma followed by rifting during the period of 2300–2400 Ma with subsequent collision at 1800–2000 Ma representing the final cratonization event.

To the south of the North China Craton lies the Qinling–Dabie–Sulu high- to ultrahigh-pressure metamorphic belt, which extends east–west for ca. 2000 km and contains diamond- and coesite-bearing eclogite [27]. This belt was formed by Triassic collision between the North China and Yangtze cratons with peak metamorphism at 245 Ma [28]. Exsolution of clinopyroxene, rutile and apatite in eclogites from Yangkou in the Sulu ultrahigh-pressure metamorphic belt suggests possible subduction of continental material to depths greater than 200 km [29].

The North China craton experienced widespread tectonothermal reactivation during the Late Mesozoic and Cenozoic, as indicated by emplacement of voluminous Late Mesozoic granites and extensive Tertiary volcanism of alkaline basalt carrying abundant mantle xenoliths. The Late Mesozoic granite magmatism is associated with widespread hydrothermal ore deposits and constitutes the most important ore-forming episode in all of Eastern China.

Diamondiferous kimberlites erupted in the Ordovician in the North China craton and occur mainly in Mengyin, Shandong Province and Fuxian, Liaoning Province (Fig. 1) [15,30,31]. In both localities the geotherm was relatively cool (36–40 mW/m<sup>2</sup>) and the lithosphere thick (ca. 200 km) at the time of eruption. The dominant xenolith type is harzburgite (*sensu stricto*). These features are characteristic of mantle beneath Archean cratons and indicate that an Archean lithospheric keel existed beneath both areas at least until eruption of the kimberlites in the Ordovician. In contrast, mantle xenoliths from Tertiary basalts are shallow and hot (800–1000°C) and consist predominantly of fertile spinel peridotite. The high temperatures are consistent with the average present-day measured surface heat flow of 60 mW/m<sup>2</sup> [32,33] and with several lines of geophysical data indicating the thickness of lithosphere varies between 120 and 50 km in the eastern part of the North China craton [15]. The above contrast between Ordovi-

cian and Tertiary mantle samples suggests that at least 80–140 km of Archean lithosphere has been removed from the base of the eastern North China craton [14,15].

### 3. Samples and localities

The xenoliths investigated in this study come from four localities of differing eruption ages and host compositions (Fig. 1): (1) Ordovician kimberlites of the Fuxian complex, which erupted on the Liaodong Peninsula, Liaoning Province [15,31], (2) the Ordovician Mengyin kimberlite complex, Shandong Province [30], (3) the Plio–Pleistocene Qixia nephelinites, Shandong Province, and (4) the 10–22 Ma Hannuoba basalts from Hebei Province. All localities occur within the North China craton: Fuxian, Mengyin and Qixia in the Eastern Block and Hannouba in the Trans-North China Orogen (Fig. 1). A brief description of each locality and the nature of the entrained xenoliths are provided below. Complete major element compositions of whole rocks and mineral phases as well as petrography and thermobarometry will be provided in a separate paper (Rudnick et al., in preparation).

#### 3.1. Fuxian

The diamondiferous Fuxian kimberlites erupted ~460 Ma ago [30] through the Archean (2900–2500 Ma) Anshan terrain [31]. The two xenoliths examined here, from pipe #50, have coarse-granular texture and are strongly serpentized and carbonated, which is reflected in their very high loss of ignition values (17–27%) and CaO contents (11.5–17.5%). Both rocks have relatively low Mg# (88–89, Table 1) compared to coarse-granular peridotites from other Archean cratons (Mg# 92–93, Fig. 2) [34]. Due to the lack of primary minerals, *P–T* conditions were not determined. However, the presence of garnet suggests minimum derivation depths of 50 km [35] and probably closer to 100 km, based on the observed spinel–garnet transition in the Kaapvaal craton [36].

## 3.2. Mengyin

The Mengyin kimberlites are also diamondiferous and erupted through the Archean to Paleoproterozoic (2700–2300 Ma) Taishan terrain [31] west of the Tan-Lu fault (Fig. 1). The peridotite xenolith investigated here has a porphyroclastic texture and comes from the Shengli #1 pipe, which has an eruption age of  $\sim 460$  Ma based on U–Pb dating of perovskite [30]. Like the Fuxian samples, this xenolith is strongly serpentinized

(LOI = 13 wt%), and no primary minerals are preserved. Paradoxically, the whole rock Mg# of this sample is high (92.2, Table 1; Fig. 2), approaching values of coarse-granular peridotites from other cratons, and distinctly higher than the Mg# of most porphyroclastic peridotites from elsewhere (e.g., [37]). As with the Fuxian samples, thermobarometry was not performed due to the poor preservation of primary phases, but minimum derivation depths of 50–100 km can be inferred.

Table 1  
Re–Os and other data for peridotite xenoliths from the North China craton

	Re (ng/g)	Os (ng/g)	$^{187}\text{Re}/^{188}\text{Os}$	$^{187}\text{Os}/^{188}\text{Os}$	$2\sigma$	$T_{\text{RD}}$ (Ga)	$T_{\text{MA}}$ (Ga)	Mg# (W.R.)	Fo	Cr# Spinel	S <sup>b</sup> (ppm)	Al <sub>2</sub> O <sub>3</sub> <sup>a</sup> (wt%)	MgO <sup>a</sup> (wt%)
Qixia													
Q1	0.094	2.526	0.1785	0.12672	22	0.40	0.67	89.7	90.3	12.3	72	2.60	40.6
Q4	0.109	1.570	0.3346	0.12992	28	future	future	89.8	89.9	8.7	66	3.58	39.2
Q5	0.014	0.843	0.0805	0.12412	21	0.75	0.93	90.9	91.0	24.8	26	1.63	44.4
Q6	0.109	7.150	0.0734	0.12000	10	1.32	1.58	91.1	91.3	47.6		1.04	46.0
		9.251		0.11992	27	1.33	1.33						
Q8	0.008	2.285	0.0167	0.12660	17	0.41	0.43	90.8	90.9	37.8	65	1.47	43.1
Q17	0.046	0.660	0.3370	0.12804	20	0.22	0.97	89.1	89.5	8.1	38	3.46	39.0
	0.048	0.544	0.4301	0.12863		0.13	17.35						
QX-07	0.098	2.230	0.2109	0.12570	9	0.54	1.04	90.0	90.2	9.7	18	3.50	41.2
		2.009		0.12539	9	0.58							
QX-11	0.146	2.765	0.2547	0.12440	11	0.72	1.73	90.0	90.0	10.2	9	3.03	41.4
QX-13	0.190	3.434	0.2662	0.12433	22	0.73	1.87	90.0	90.2	12.7		3.15	40.8
QX-14	0.040	4.277	0.0455	0.12606	14	0.49	0.55	91.1	90.4	9.2		2.17	42.2
Hannuoba													
DMP 04	0.198	3.954	0.2412	0.12353	14	0.84	1.87	91.1	91.1	16.8	73	2.29	42.7
	0.198	3.935	0.2427	0.12314	7	0.89	2.00						
DMP 19	0.108	4.350	0.1189	0.12026	19	1.28	1.76	91.1	91.3	24.5	91	1.91	42.1
DMP 23A	0.075	3.472	0.1043	0.11878	18	1.48	1.94	90.4	91.1	27.1		2.32	42.2
DMP 25	0.032	3.256	0.0476	0.11664	12	1.77	1.99	91.7	91.6	36.0	20	1.61	44.5
DMP 41	0.158	2.923	0.2599	0.12358	19	0.83	2.05	90.2	90.4	12.8	110	2.76	40.7
DMP 51	0.138	3.492	0.1903	0.12357	12	0.83	1.47	91.0	91.1	20.2	130	1.96	42.3
DMP 56	0.229	3.746	0.2947	0.12769	7	0.26	0.82	89.5	89.9	9.1	260	3.49	38.6
	0.232	3.642	0.3080	0.12819	66	0.20	0.67						
DMP 58	0.185	3.954	0.2253	0.12591	16	0.51	1.06	89.7	90.2	10.8	230	3.16	39.3
DMP 59	0.231	4.654	0.2387	0.12377	21	0.80	1.78	90.0	90.4	14.0	200	2.58	40.97
DMP 60	0.292	4.187	0.3359	0.12668	13	0.40	1.78	89.7	90.1	9.3	320	3.67	37.1
	0.293	4.097	0.3450	0.12644	9	0.44	2.11						
DMP 67c	0.040	1.879	0.1026	0.12333	9	0.86	1.13	88.9	89.5	9.9	23	3.78	38.7
Fuxian													
F50-9270	0.015	1.200	0.0620	0.11011	11	2.70	3.07	89.0				0.96	30.4
	0.015	1.145	0.0631	0.11136	31	2.53	2.89						
F50-9271	0.026	1.724	0.0705	0.10919	7	2.83	3.29	88.5				1.54	27.5
Mengyin													
SD 9405	0.2869	2.879	0.4800	0.12216	12	1.46	future	92.2				0.72	44.5

<sup>a</sup> Normalized to 100% volatile-free.

<sup>b</sup> Missing S data for Qixia samples represent those too small to obtain sulfur data.

Values of PUM ( $^{187}\text{Os}/^{188}\text{Os}=0.1296$  and  $^{187}\text{Re}/^{188}\text{Os}=0.433$  [66]) (used for the calculation of  $T_{\text{RD}}$  and  $T_{\text{MA}}$  ages).

### 3.3. Qixia

The Qixia nephelinite erupted  $\sim 6$  Ma ago in the Shandong peninsula, to the east of the Tan-Lu fault (Fig. 1) [16]. Although there has been some recent debate about where the North China–Yangtze boundary cuts through this peninsula [38–40], the presence of 2800 Ma TTG and granitic gneiss basement in the Qixia area [21,41] confirms that this region is part of the North China craton.

Qixia xenoliths are coarse-grained, small (1–4 cm) spinel lherzolites and are contained completely within the nephelinite host. The combination of small sample size and coarse grain size compromises whole rock compositions (see below). These lherzolites are generally very fresh, although clinopyroxene breakdown is observed near the contacts with the host lava. Sulfides are rare to absent in these xenoliths, consistent with their low S abundances (10–70 ppm) and lack of correlation between S and MgO (Fig. 3). Such depletions are common in upper mantle xenoliths due to sulfide breakdown, which may occur due to rapid decompression [42] or pre-entrainment oxidation. Major element compositions vary somewhat ( $Mg\# = 89\text{--}91$ , Table 1; Fig. 2), indicating variable degrees of melt depletion. Qixia

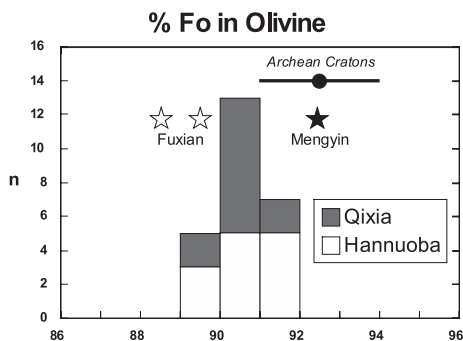


Fig. 2. Histogram of forsterite content ( $\%Fo = 100 \times Mg / (Mg + Fe)$ , where Mg and Fe represent molar proportions) of olivines from peridotite xenoliths from Qixia and Hannuoba. Open and closed stars represent whole rock  $Mg\#$  for the Fuxian and Mengyin kimberlite-hosted peridotites, respectively. Bar with circle at the top of diagram represents average and typical range of Fo contents of olivines from typical Archean cratons such as Kaapvaal, Siberia, Tanzania and eastern Greenland (see [8] for data sources).

is more refractory than other peridotite xenoliths from Cenozoic basalts in the Shandong peninsula (e.g., Shanwang locality [16]), but the very refractory compositions typical of peridotites from Archean cratons (e.g., [34]) and observed in the Mengyin peridotite are not present at Qixia (Fig. 3, and [16]). The samples yield pyroxene temperatures between 840 and 980°C (Rudnick et al., in preparation); derivation depths are only broadly constrained by the depth of the Moho (35 km), and the transition between spinel and garnet facies peridotites (60 km, based on O’Neill’s [35] data and a minimum Cr# of 10).

### 3.4. Hannuoba

Hannuoba xenoliths were collected from lava flows at the Damaping locality [43,44], which erupted through the Archean Huai’an terrain. A variety of xenolith types occur at Hannuoba (mafic and felsic granulites, spinel- and garnet-bearing pyroxenites, spinel lherzolites and rare garnet–spinel lherzolites), and these have been the subject of a number of geochemical and petrological studies [44–47].

Hannuoba peridotite xenoliths are generally large (up to 50 cm) and are very fresh. An unusual feature of these xenoliths is the large amount of sulfides that are present. These occur mainly as tiny (5–10  $\mu m$ ) inclusions within glass that coats grain boundaries, but also as larger grains at triple junctions (20–40  $\mu m$ ), decorating healed fractures within silicates, and as large (50–70  $\mu m$ ), isolated inclusions. The preservation of sulfides in these xenoliths is reflected in the bulk rock S contents, which range between 20 and 320 ppm (Table 1), and correlates well with major element composition for all but one sample (Fig. 3). The Hannuoba xenoliths display a similar range in  $Mg\#$  (89–92) and major element composition similar to that of the Qixia xenoliths (Fig. 3), indicating similar degrees of melt extraction. In contrast to Qixia, Hannuoba peridotites examined here record equilibration temperatures between 940 and 1050°C, with all but one above 1000°C, and are thus significantly hotter than the Qixia peridotites. Comparing these temperatures to the  $P$ – $T$  array derived from Hannuoba garnet pyroxenites

[46] yields derivation depths between 40 and 55 km for the spinel lherzolites, comparable to the depth range estimated for the Qixia peridotites.

#### 4. Analytical techniques

The xenoliths were sawn from their lava hosts and the cut surfaces were abraded with quartz in a sand blaster to remove any possible contamination from the saw blade. The samples were then disaggregated between thick plastic sheets with a rock hammer and reduced to powder using first an alumina disk mill followed by an alumina ring mill.

Major element compositions were determined by XRF on fused glass disks at the University of Massachusetts at Amherst [68] and Northwest University in Xi'an, China. Sulfur analyses were carried out by Leco spectrophotometry at the University of Leicester (see [48] for details). Complete major element compositions will be reported in Rudnick et al. (in preparation).

Re–Os procedures followed those detailed in Carlson et al. [49], which includes Carius tube digestions of approximately 1 g of sample using a mixed Re–Os spike, followed by Os extraction and Re purification on anion exchange columns. Re and Os were loaded onto Pt filaments with  $\text{Ba}(\text{NO}_3)_2$  as an activator and analyzed as negative ions using the DTM 15-inch mass spectrometer (see [11] for details). Total procedural blanks did not exceed 2.0 pg for both Os and Re. These blanks are inconsequential for Os, but are significant for the lower Re samples, consequently blank corrections were made to all samples using an average Re blank of  $1 \pm 0.5$  pg. Replicate analyses performed on separate dissolutions are within analytical uncertainty for  $^{187}\text{Os}/^{188}\text{Os}$  for all but one sample (DMP 04), but replicate Os concentrations all vary beyond analytical uncertainty ( $\pm 2\%$ ), indicative of inadequate sampling of the whole rock (the so-called nugget effect).

#### 5. Re–Os systematics

Determining the age of lithospheric mantle

would provide critical evidence to test the lithosphere removal hypothesis and may elucidate the timing and processes involved. Lithospheric mantle is typically chemically depleted relative to the convecting mantle, which results in increased buoyancy, viscosity, thickness and hence strength of the lithospheric mantle. We take this as evidence that the lithospheric mantle grows by melt extraction rather than by simple conductive cooling. The Re–Os isotopic system can be used to date melting events in peridotites, since Re is moderately incompatible and Os is strongly compatible. Melting lowers the Re/Os of the residue and Os isotopic growth will be retarded relative to convecting mantle. The Re–Os systematics can thus be used to date lithospheric mantle growth in several ways, which we summarize below.

A Re–Os isochron will develop if the peridotites underwent melt extraction from the same mantle source at the same time, and no Re or Os mobility has occurred subsequent to melting. However, mantle xenoliths often exhibit evidence of Re mobility in the form of Re introduction from the host magma or through mantle metasomatic processes (e.g., [48,50]), or Re loss due to sulfide breakdown [51]. Coupled with the possibility of multiple sources and melting events, Re mobility means that Re–Os isochrons are rarely observed for peridotite xenolith suites.

One way to circumvent the problem of Re mobility is to plot  $^{187}\text{Os}/^{188}\text{Os}$  against an immobile element that exhibits a similar degree of incompatibility as Re during mantle melting. Elements meeting this criterion include  $\text{Al}_2\text{O}_3$ , CaO, HREE and Y (e.g., [51,52]). If the data form a positive trend, then the  $^{187}\text{Os}/^{188}\text{Os}$  of the intercept [52] or the  $^{187}\text{Os}/^{188}\text{Os}$  present at the lowest likely  $\text{Al}_2\text{O}_3$  concentration (e.g., 0.5 wt%  $\text{Al}_2\text{O}_3$ ) [53] can be used as the initial ratio, and this ratio compared to a model mantle evolution trend to determine the time of melting.

Alternatively, the time of melt depletion can be determined for individual peridotites by using the observed Re/Os ratio and calculating when the sample had a  $^{187}\text{Os}/^{188}\text{Os}$  matching primitive upper mantle ( $T_{\text{MA}}$  ages [50]). These model ages are completely analogous to Sm–Nd model ages

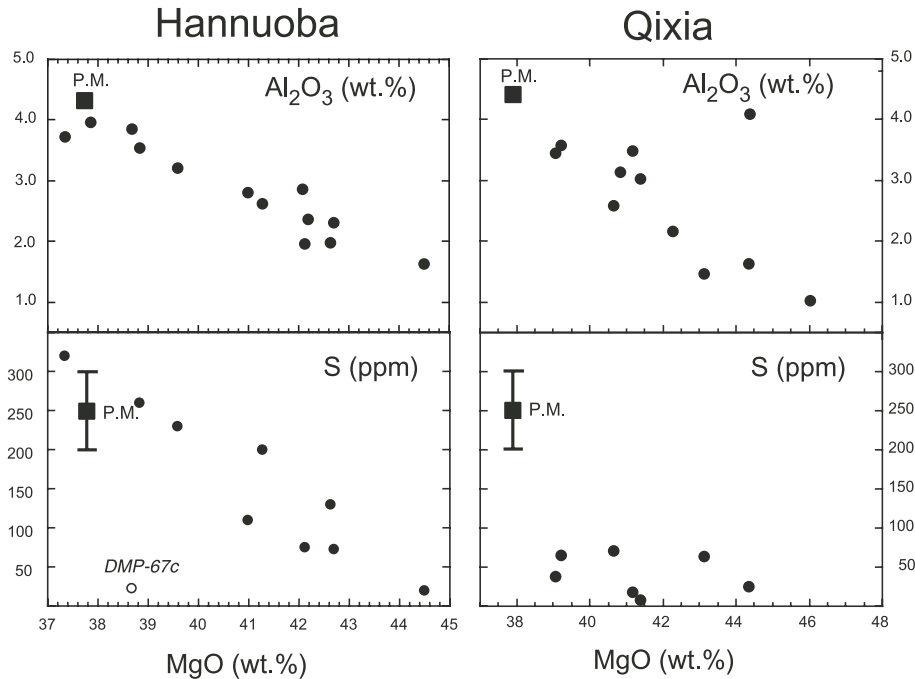


Fig. 3. Whole rock S and  $\text{Al}_2\text{O}_3$  vs. MgO contents for Qixia and Hannuoba peridotites. The black square labelled 'P.M.' in each diagram is the primitive mantle composition from McDonough and Sun [65]. Of the elements plotted, sulfur is the least well constrained in the primitive mantle and it is shown with error bars from [65]. Sulfur correlates well with MgO for the Hannuoba xenoliths (except sample DMP 67c, plotted as an open circle), but poorly for the Qixia xenoliths, reflecting the excellent preservation of sulfides in the former. One Qixia sample falls high and off the  $\text{Al}_2\text{O}_3$  vs. MgO trend. This is attributed to preferential sampling of spinel in this small sample; its CaO content is not anomalous compared to the other samples. This sample was not measured for Os isotopes.

(e.g., [54]), but rely on Re immobility, which is often a problem for mantle xenoliths, as discussed above.

Another method, which provides a minimum estimate of the timing of melt depletion, is simply to compare the  $^{187}\text{Os}/^{188}\text{Os}$  of the sample corrected using the measured Re/Os to the time of xenolith host eruption to a mantle evolution model. The time at which the mantle had this  $^{187}\text{Os}/^{188}\text{Os}$  composition is referred to as the  $T_{\text{RD}}$ , or 'Re-depletion' age [50]. If all of the Re was removed at the time of melting, then the  $T_{\text{RD}}$  age should equal the  $T_{\text{MA}}$  age (assuming no Re addition).  $T_{\text{RD}}$  ages are good approximations to the time of melting for highly refractory peridotites, such as cratonic xenoliths, but in less refractory material, where some Re remains in the residue,  $T_{\text{RD}}$  ages are minimum ages.

## 6. Results

Chemical and isotopic data are reported in Table 1 for the Chinese peridotites. Os contents of the Qixia lherzolites vary widely from 0.5 to 9 ppb, whereas Os contents of the Hannuoba lherzolites fall into a more restricted range, between 1.9 and 4.6 ppb. The three peridotites from the kimberlites lie on the low side of this concentration range at 1.2–2.9 ppb, overlapping a number of Qixia samples (Fig. 4) and having similar concentrations to cratonic peridotites from Siberia and Wyoming. Re contents of the Qixia samples overlap those of Hannuoba, but are in general more depleted in Re (Fig. 4). Both suites have Re contents at or below primitive mantle concentrations, consistent with variable Re loss through melt depletion and inconsistent with exchange

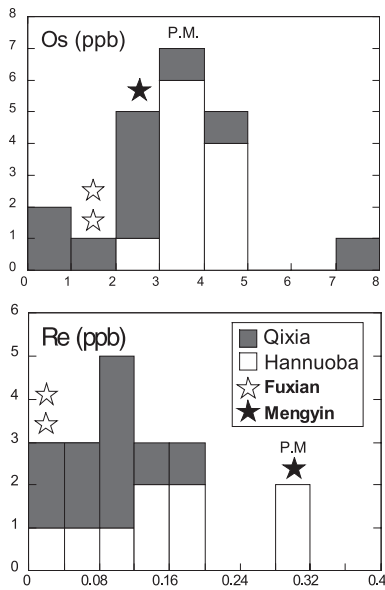


Fig. 4. Histograms of Os and Re contents for the Chinese peridotites investigated here. 'P.M.' is primitive mantle value from McDonough and Sun [65].

with the host lava, which should impart high Re/Os on the xenolith. There is no evidence for Re re-enrichment, as has been observed in some cratonic peridotites [48]. The sample from the Mengyin kimberlite has a relatively high Re content, whereas both samples from Fuxian are strongly depleted in Re.

The two garnet peridotites from the Fuxian kimberlite have Archean  $T_{RD}$  and  $T_{MA}$  ages (2500–2800 Ma and 2900–3300 Ma, respectively; Fig. 5 and Table 1). In contrast, the Mengyin garnet peridotite has a Proterozoic  $T_{RD}$  age (1500 Ma, Fig. 5). The  $T_{MA}$  age of this sample is negative (in the future), due to its superchondritic  $^{187}\text{Re}/^{188}\text{Os}$ .

The  $^{187}\text{Os}/^{188}\text{Os}$  for all but one of the Qixia xenoliths varies within a rather narrow range of 0.1241–0.1299, overlapping the  $^{187}\text{Os}/^{188}\text{Os}$  of PUM (primitive upper mantle as estimated from world-wide mantle xenoliths [55]) and abyssal peridotites (Fig. 6). Sample Q6, which is the most refractory and has an unusually high Os concentration (7–9 ppb), has a significantly lower  $^{187}\text{Os}/^{188}\text{Os}$  of 0.1200. Major element compositions of the Qixia peridotites are compromised

by the very small sample size, as witnessed by one sample plotting far off the apparent melt depletion trend observed between  $\text{MgO}$  and  $\text{Al}_2\text{O}_3$  (Fig. 3). For this reason, mineral compositions are more robust indicators of the degree of melt depletion in this xenolith suite. There is a very poor correlation between  $^{187}\text{Re}/^{188}\text{Os}$  and  $^{187}\text{Os}/^{188}\text{Os}$  (Fig. 6), as well as olivine Fo content vs.  $^{187}\text{Os}/^{188}\text{Os}$  ( $r=0.5$ ) or spinel Cr# vs.  $^{187}\text{Os}/^{188}\text{Os}$  for the Qixia samples ( $r=0.4$ , Fig. 7). There is a much better correlation between  $^{187}\text{Re}/^{188}\text{Os}$  and olivine forsterite content ( $r=0.74$ ). There is no correla-

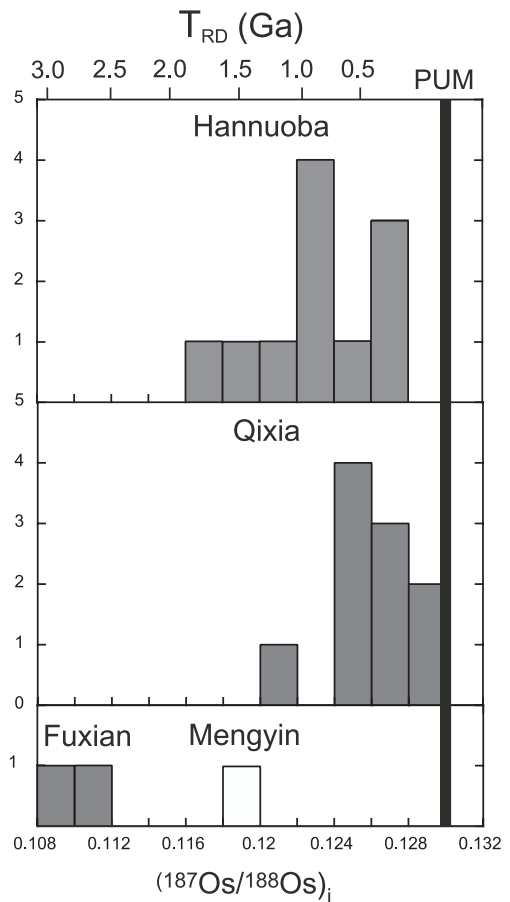


Fig. 5. Histogram of  $^{187}\text{Os}/^{188}\text{Os}$  for the xenoliths at the time of eruption. 'PUM' is primitive upper mantle composition of Meisel et al. [55]. Upper scale gives Re-depletion ( $T_{RD}$ ) model ages in billions of years. Top, middle and lower panels are Hannuoba, Qixia and kimberlite-hosted xenoliths from Fuxian and Mengyin, respectively.

tion between Os isotopic composition and temperature (hence derivation depth).

In contrast to the Qixia peridotites,  $^{187}\text{Os}/^{188}\text{Os}$  of the Hannuoba xenoliths varies from 0.117 to 0.128 and correlates well with  $^{187}\text{Re}/^{188}\text{Os}$  (Fig. 6),  $\text{Al}_2\text{O}_3$  ( $r=0.73$ ),  $\text{CaO}$  ( $r=0.86$ ),  $\text{Mg\#}$  ( $r=0.67$ ) and spinel  $\text{Cr\#}$  ( $r=0.94$ ; Fig. 7).  $T_{\text{RD}}$  ages range from 200 to 1800 Ma (Figs. 5 and 6) and  $T_{\text{MA}}$  ages range from 700 to 2100 Ma (Table 1), with most falling within the range of 1500–2000 Ma, consistent with their near isochronous relationship (Fig. 6). However, like Qixia, there is no correlation between equilibration temperature and Os isotopic composition.

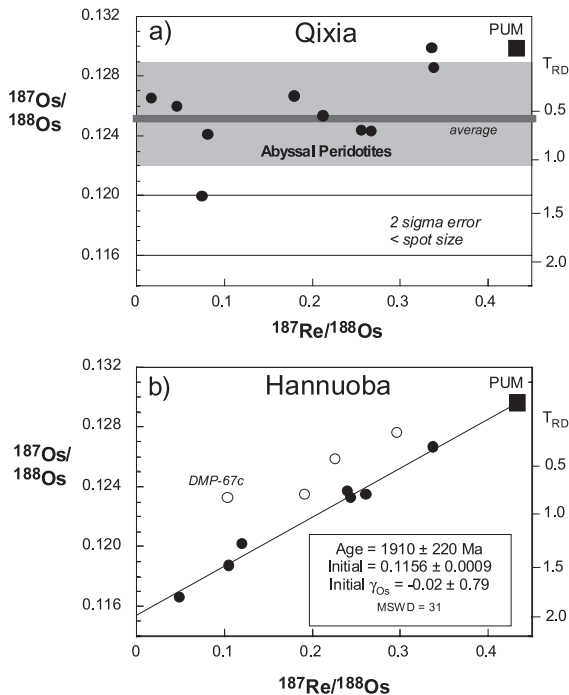


Fig. 6. Re–Os isochron diagrams for Chinese peridotites. Black square represents primitive upper mantle (‘PUM’) [55]. (A) Qixia peridotites. Shaded field represents range of  $^{187}\text{Os}/^{188}\text{Os}$  in abyssal peridotites (see Brandon et al. [66] and references therein) and dark gray line represents the average abyssal peridotite (from [66]). (B) Hannuoba peridotites. Sample DMP 67c (labelled open symbol) shows evidence for sulfide breakdown (see text). The other three open circles are eliminated from the regression if the isochron is forced through estimates of present-day PUM. Data regressed and MSWD determined using Isoplot program of Ludwig [67].

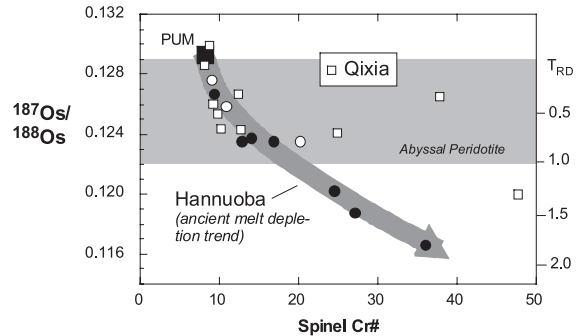


Fig. 7. Spinel  $\text{Cr\#}$  [ $100 \times \text{Cr}/(\text{Cr}+\text{Al})$ ] versus  $^{187}\text{Os}/^{188}\text{Os}$  for Qixia (white squares,  $r=0.4$ ) and Hannuoba peridotites (black circles,  $r=0.94$ ). White circles represent the three Hannuoba samples excluded from the isochron in Fig. 6. Whereas Hannuoba peridotites define an ancient melting trend, Qixia samples show only a poor correlation between  $\text{Cr\#}$  and  $^{187}\text{Os}/^{188}\text{Os}$ , consistent with them representing residues from recent melting of a heterogeneous upper mantle source. In particular, the Qixia samples with high  $\text{Cr\#}$  and relatively high  $^{187}\text{Os}/^{188}\text{Os}$  must have experienced melt depletion recently. Field of abyssal peridotites as in Fig. 6.

## 7. Discussion

### 7.1. Phanerozoic lithosphere replacement beneath the Eastern Block of the North China craton

The limited Re–Os data for kimberlite-hosted garnet peridotites from Fuxian and Mengyin document the presence of ancient lithosphere beneath the Eastern Block of the North China craton during the Ordovician. The Fuxian xenoliths are clearly Archean, with both  $T_{\text{RD}}$  and  $T_{\text{MA}}$  ages greater than 2500 Ma. The low Re in these samples may well be a primary feature and suggests that intensive serpentinization does little to increase the Re/Os or alter  $^{187}\text{Os}/^{188}\text{Os}$  of peridotite xenoliths. In contrast, the Mengyin peridotite has significantly higher Re/Os and a younger  $T_{\text{RD}}$  age. The future  $T_{\text{MA}}$  age indicates that this sample experienced Re addition significantly after the original melt depletion event that gave rise to its refractory composition. Because the  $T_{\text{RD}}$  age is Proterozoic, Re addition may have occurred either at the time of kimberlite magmatism (and the  $T_{\text{RD}}$  age reflects the time of melt depletion), or significantly before kimberlite magmatism (e.g., at 1300 Ma, assuming that melt depletion oc-

curred in the Archean and that the original residual peridotite had no Re). The latter scenario is more likely considering the very refractory composition of this peridotite, which is similar to Archean cratonic mantle lithosphere [34]. In either case, the mid-Proterozoic model age for this sample provides a minimum age of melt depletion, indicating that the lithosphere beneath Mengyin is Proterozoic or older.

In contrast to these ancient ages, the Qixia peridotites generally have young  $T_{RD}$  and  $T_{MA}$  ages (0–700 Ma), with one sample significantly older (Q6 with  $T_{RD}$  and  $T_{MA}$  of 1300 and 1600 Ma, respectively). The samples define very poor correlations on a Re–Os isochron plot (Fig. 6a), which could reflect: (1) recent melt extraction, so the Os isotopic composition has not had time to evolve to match Re/Os ratio, (2) disturbed Re (and/or Os) contents, (3) derivation of the xenoliths from a source with heterogeneous  $^{187}\text{Os}/^{188}\text{Os}$  and/or (4) Os isotopic compositions that have been overprinted by sulfide metasomatism. We favor a combination of the first and third possibilities.

The relatively good correlation between Re/Os ratio and indicators of melt depletion such as olivine forsterite content or spinel Cr# suggests that Re and Os have not been significantly disturbed by post-melting processes (such as sulfide metasomatism and sulfide breakdown). This inference, coupled with the poor correlation between  $^{187}\text{Os}/^{188}\text{Os}$  and these same indicators of melt depletion (e.g., Fig. 7), is consistent with the peridotites forming by recent partial melt extraction from a source region with heterogeneous  $^{187}\text{Os}/^{188}\text{Os}$ . (Note that it is not appropriate to plot these samples on an  $\text{Al}_2\text{O}_3$ – $^{187}\text{Os}/^{188}\text{Os}$  plot considering their very small size and consequent compromised major element compositions, as described above.)

Recent work has documented that whole rock Os isotopic compositions may be changed to variable degrees by addition of radiogenic Os in metasomatic sulfides [48,56–58]. Such addition is usually accompanied by a significant increase in Re/Os ratio [56,57], but this is not observed in the Qixia samples. Moreover, secondary sulfides are reported to have one to two orders of magnitude

lower Os content than primary sulfides [59], which means that large additions of metasomatic sulfides are required in order to accomplish significant shifts in whole rock Os isotope compositions. For example, if the Qixia samples are Archean peridotites that have been overprinted by radiogenic Os, 50–100% of the current Os in the samples must derive from metasomatic sulfide (assuming a  $^{187}\text{Os}/^{188}\text{Os}$  of 0.1296 for metasomatic sulfide and a starting  $^{187}\text{Os}/^{188}\text{Os}$  of 0.1156). Taking just the lower limit would correspond to a ratio of metasomatic sulfide to primary sulfide of 10:1 to 100:1. The Qixia samples contain very low S contents and rare sulfides – if present originally, they have been lost by decomposition. Collectively, these observations rule out the possibility that the Qixia peridotites are Archean residues overprinted by recent metasomatism.

The wide range in fertility of the Qixia xenoliths (as displayed, for example by the bulk rock Mg#, olivine Fo content and spinel Cr#), coupled with a range in  $^{187}\text{Os}/^{188}\text{Os}$  similar to modern oceanic peridotites (minus sample Q6), suggests that the lithospheric mantle beneath this portion of the Shandong Peninsula formed recently from the convecting mantle. This observation, coupled with the ancient ages from Ordovician kimberlite-borne xenoliths demonstrates nicely that the ancient lithosphere that once underlay this region of the craton has been removed and replaced by younger material, as suggested by previous workers [14–16,60].

The lack of correlation between temperature (hence derivation depth) and bulk composition or  $^{187}\text{Os}/^{188}\text{Os}$  for the Qixia samples demonstrates that the lithospheric mantle is not stratified with respect to either composition or age. In this respect, lithospheric replacement beneath the North China craton differs from that observed beneath the Sierra Nevada, California, where a thin veneer of ancient lithosphere is still preserved just beneath the Moho [61]. If the single unradiogenic Qixia sample is a relict of the earlier lithosphere, it appears to be a minor component dispersed within the younger lithosphere, as its equilibration temperature is one of the highest observed for Qixia, implying this xenolith was derived from one of the deepest regions sampled. Alternatively,

this sample may simply reflect the heterogeneity that exists in Os isotopic composition within modern convecting mantle. For example, peridotites with similarly unradiogenic  $^{187}\text{Os}/^{188}\text{Os}$  (down to 0.1193) have been described from the forearc of the Izu–Bonin arc [62] and the central Atlantic [63] and are attributed to small scale heterogeneity within convecting mantle.

Because of the large uncertainty in Os model ages for Qixia samples due to the lack of an isochron or good correlations between  $^{187}\text{Os}/^{188}\text{Os}$  and indicators of fertility (Mg#, spinel Cr#, etc.) and the likely heterogeneity of  $^{187}\text{Os}/^{188}\text{Os}$  in the convecting mantle, it is not possible to constrain the timing of formation of the ‘new’ lithosphere from the Re–Os data beyond the observation that it is less than  $\sim 1000$  Ma. Because Archean lithosphere was present in the region at the time of kimberlite magmatism, as evidenced by the Fuxian and Mengyin samples, the lithosphere sampled by the Qixia activity must be younger than Ordovician. Geological evidence points strongly to lithosphere removal being associated with the Mesozoic collision of the Yangtze and North China cratons along the Qinling–Dabie–Sulu high- to ultrahigh-pressure metamorphic belt. Unlike other Archean cratons, the North China craton experienced significant tectono-thermal reactivation after its Triassic collision with the Yangtze Craton. This is well illustrated by:

1. intensive granite magmatism, mafic–felsic volcanism and associated hydrothermal mineralization in the Jurassic and Cretaceous,
2. transformation of tectonic deformation direction from east–west to north–west at the Jurassic–Cretaceous transition,
3. strong extension and large basin formation in the Jurassic to Tertiary, and
4. widespread eruption of continental rift-related alkaline basalts in the Tertiary.

These observations suggest that removal of older lithosphere and formation of the ‘new’ lithosphere most likely occurred in the Jurassic and Cretaceous [64]. The processes may have been triggered by the Triassic collision [64] and accompanied by lower crustal foundering in the North China Craton [32].

## 7.2. Precambrian lithosphere replacement beneath the Trans-North China Orogen

The Hannuoba peridotites display one of the best Re–Os isochrons yet reported for a suite of upper mantle xenoliths. This may be due to the preservation of sulfides in these samples. One sample (DMP 67c) has clearly experienced sulfide breakdown, based on its very low S content (20 ppm) at an MgO content approaching that of the primitive mantle (Fig. 3) and the paucity of sulfides in thin section. This sample plots off the S–MgO correlation defined by the rest of the Hannuoba samples (Fig. 3), and has a low Re/Os ratio. Excluding this sample from the Re–Os isochron yields an ‘errorchron’ age of  $2082 \pm 540$  Ma, an initial  $\gamma_{\text{Os}}$  of  $+1.5 \pm 2.0$  and an MSWD of 408. The elevated and uncertain initial ratio is eliminated if the regression line is forced through a bulk Earth Re–Os model (PUM in Fig. 6b). This causes the data for three additional samples to plot off the best-fit line in the direction of recent Re loss. Excluding these three points from the regression lowers the isochron age to  $1910 \pm 220$  Ma, with a lower MSWD (35) and initial  $\gamma_{\text{Os}}$  of  $-0.02 \pm 0.79$ . This is our preferred age for formation of the lithospheric mantle beneath Hannuoba.

It is interesting to note that despite what appear to be multiple generations of sulfides in these samples, the Re–Os systematics appear to be unperurbed. This may suggest that texturally ‘secondary’ sulfides (i.e., on grain boundaries and in fractures) simply represent remobilized primary sulfides (based on two-pyroxene thermometry, the xenoliths resided at temperatures above the sulfide solidus in the lithospheric mantle). Alternatively, and perhaps more likely, the Os content of the secondary sulfides is too low to change the whole rock Os isotopic composition appreciably, as discussed above.

The Re–Os data for the Hannuoba xenoliths suggest the present mantle lithosphere formed at  $1900 \pm 220$  Ma. Although we cannot determine from our data the mechanism responsible for lithosphere removal and replacement, the time constraints do provide some insight. The region has undergone both rifting (2400–2300 Ma) and

continent–continent collision (2000–1800 Ma) [20,22], both of which may have led to mantle lithosphere replacement. If rifting was responsible for removal of the original ~2700 Ma lithospheric mantle, then there appears to have been a hiatus of 200–700 Ma between its removal and formation of the current mantle lid. In contrast, the timing of new lithosphere formation is coincident with that of continent–continent collision. We assume that continental crust cannot exist for long periods of time in the absence of an insulating mantle lid. If this is true, and if the ages above are indeed robust, it suggests that collision, rather than rifting, was most likely responsible for the replacement of mantle lithosphere. Further high-precision geochronology on crustal rocks and additional Re–Os data for xenolith suites are needed before firm conclusions can be made.

## 8. Conclusions

The main conclusions to be drawn from the Re–Os data presented here are as follows.

1. Archean lithosphere existed beneath the Eastern Block of the North China craton in the Ordovician.
2. No trace of Archean lithosphere was found in mantle xenoliths from Qixia, which lies about 250 km from the kimberlites, in Archean rocks of the Shandong peninsula.
3. The mantle lithosphere sampled by Tertiary basalts in the Trans-North China Orogen matches the age of the last major orogeny (1900 Ma) and is significantly younger than the original crust formation age (2700 Ma).
4. Two episodes of removal and replacement of Archean lithospheric mantle by less refractory peridotite are inferred.
5. Both events appear to be associated with major continent–continent collisions, one in the Proterozoic and the second in the Mesozoic.

## Acknowledgements

We thank Jianping Zheng for providing the

kimberlite xenoliths; David Lange and Phil Piccoli for assistance with microprobe analyses at Harvard and University of Maryland, respectively; Kate Tomford for sample preparation and Patricia Fiori for carrying out microprobe analyses at Harvard, and Mary Horan and Tim Mock for help with the Re–Os analyses at DTM. Review comments of Thomas Meisel, Martin Menzies and especially Laurie Reisberg helped improve the manuscript. This research was supported by NSF Grant EAR 99031591 to R.L.R. and W.F.M. and the Chinese Ministry of Science and Technology (Grant G1999043202) and the National Nature Science Foundation of China (S.G.).[AH]

## References

- [1] P. Morgan, The thermal structure and thermal evolution of the continental lithosphere, in: H.N. Pollack, V.R. Murthy (Eds.), *Structure and Evolution of the Continental Lithosphere*, Vol. 15, Phys. and Chem. Earth, 1984, pp. 107–193.
- [2] A.A. Nyblade, H.N. Pollack, A global analysis of heat flow from Precambrian terrains: implications for the thermal structure of Archean and Proterozoic lithosphere, *J. Geophys. Res.* 98 (1993) 12207–12218.
- [3] T.H. Jordan, Structure and formation of the continental lithosphere, in: M.A. Menzies, K. Cox (Eds.), *Oceanic and Continental Lithosphere; Similarities and Differences*, *J. Petrol.*, Special Lithosphere Issue, 1988, pp. 11–37.
- [4] S.P. Grand, Tomographic inversion for shear velocity beneath the North American plate, *J. Geophys. Res.* 92 (1987) 14065–14090.
- [5] F.R. Boyd, S.A. Mertzman, Composition and structure of the Kaapvaal lithosphere, southern Africa, in: B.O. Mysen (Ed.), *Magmatic Processes: Physicochemical Principles*, Special Pub. No., The Geochemical Society, 1987, pp. 13–24.
- [6] H.N. Pollack, Cratonization and thermal evolution of the mantle, *Earth Planet. Sci. Lett.* 80 (1986) 175–182.
- [7] R.W. Kay, S.M. Kay, Creation and destruction of lower continental crust, *Geol. Rundsch.* 80 (1991) 259–278.
- [8] C.-T. Lee, Q. Yin, R.L. Rudnick, S.B. Jacobsen, Preservation of ancient and fertile lithospheric mantle beneath the southwestern United States, *Nature* 411 (2001) 69–73.
- [9] S.P. Grand, Mantle shear structure beneath the Americas and surrounding oceans, *J. Geophys. Res.* 99 (1994) 11591–11621.
- [10] S. van der Lee, G. Nolet, The upper-mantle S-velocity structure of North America, *J. Geophys. Res.* 102 (1997) 22815–22838.

- [11] R.W. Carlson, A.J. Irving, Depletion and enrichment history of subcontinental lithospheric mantle: An Os, Sr, Nd and Pb isotopic study of ultramafic xenoliths from the northwestern Wyoming Craton, *Earth Planet. Sci. Lett.* 126 (1994) 457–472.
- [12] R.W. Carlson, A.J. Irving, B.C. Hearn, Chemical and isotopic systematics of peridotite xenoliths from the Williams Kimberlite, Montana: Clues to processes of lithosphere formation, modification and destruction, in: J.J. Gurney, J.L. Gurney, M.D. Pascoe, S.H. Richardson (Eds.), *The J.B. Dawson Volume. Proceedings of the VIIth International Kimberlite Conference, Red Roof Design, Cape Town, 1999*, pp. 90–98.
- [13] D.-Y. Liu, A.P. Nutman, W. Compston, J.S. Wu, Q.-H. Shen, Remnants of > 3800 Ma crust in the Chinese part of the Sino-Korean craton, *Geology* 20 (1992) 339–342.
- [14] M.A. Menzies, W.-M. Fan, M. Zhang, Paleozoic and Cenozoic lithoprobes and the loss of > 120 km of Archean lithosphere, Sino-Korean craton, China, in: H.M. Pritchard, T. Alabaster, N.B.W. Harris, C.R. Neary (Eds.), *Magmatic Processes and Plate Tectonics*, Vol. 76, Geological Society, London, 1993, pp. 71–81.
- [15] W.L. Griffin, A.D. Zhang, S.Y. O'Reilly, C.G. Ryan, Phanerozoic evolution of the lithosphere beneath the Sino-Korean Craton, in: M. Flower, S.-L. Chung, C.-H. Lo, T.-Y. Lee (Eds.), *Mantle Dynamics and Plate Interactions in East Asia*, American Geophysical Union, Washington, DC, 1998, pp. 107–126.
- [16] Z. Zheng, S.Y. O'Reilly, W.L. Griffin, F. Lu, M. Zhang, Nature and Evolution of Cenozoic Lithospheric Mantle beneath Shandong Peninsula, Sino-Korean Craton, Eastern China, *Int. Geol. Rev.* 40 (1998) 471–499.
- [17] G.C. Zhao, P.A. Cawood, S.A. Wilde, M. Sun, Metamorphism of basement rocks in the Central Zone of the North China Craton: implications for Paleoproterozoic tectonic evolution, *Precambrian Res.* 103 (2000) 55–88.
- [18] G.C. Zhao, S.A. Wilde, P.A. Cawood, M. Sun, Archean blocks and their boundaries in the North China Craton: lithological, geochemical, structural and P-T path constraints and tectonic evolution, *Precambrian Res.* 107 (2001) 45–73.
- [19] T.M. Kusky, J.-H. Li, R.D. Tucker, The Archean Dongwanzhi Ophiolite Complex, North China Craton 2.505-billion-year-old oceanic crust and mantle, *Science* 292 (2001) 1142–1145.
- [20] J.H. Li, G.T. Hou, X.N. Huang, Z.Q. Zhang, X.L. Qian, Constraints on the supercontinental cycles: Evidence from Precambrian geology of North China Craton, *Acta Petrol. Sin.* 17 (2001) 177–186 (in Chinese).
- [21] J.S. Wu, Y.S. Geng, Q.H. Shen, Y.S. Wan, D.Y. Liu, B. Song, Archean Geology and Tectonic Evolution of the North China Craton (in Chinese), Geological Publishing House, Beijing, 1998, 212 pp.
- [22] J.H. Li, X.L. Qian, X.N. Huang, S.W. Liu, Tectonic framework of the North China Craton and its cratonization in the early Precambrian, *Acta Petrol. Sin.* 16 (2000) 1–10 (in Chinese).
- [23] A. Kröner, W. Compston, G. Zhang, A. Guo, W. Cui, Single grain zircon ages for Archean rocks from Henan, Hebei and Inner Mongolia, China and tectonic implications, *Int. Symp. Tectonic Evolution and Dynamics of Continental Lithosphere, 1987* (abstract).
- [24] A. Kröner, W. Compston, G.W. Zhang, A.L. Guo, W. Todt, Ages and tectonic setting of Late Archean greenschist-gneiss terrain in Henan Province, China as revealed by single-grain zircon dating, *Geology* 16 (1988) 211–215.
- [25] H. Kern, S. Gao, Q.-S. Liu, Seismic properties and densities of middle and lower crustal rocks exposed along the North China Geoscience Transect, *Earth Planet. Sci. Lett.* 139 (1996) 439–455.
- [26] K.C. Condie, *Plate Tectonics and Crustal Evolution*, Butterworth-Heinemann, Oxford, 1997, 282 pp.
- [27] S. Xu, A.I. Okay, S. Ji, A.M.C. Sengör, W. Su, Y. Liu, L. Jiang, Diamond from the Dabie Shan metamorphic rocks and its implication for tectonic setting, *Science* 256 (1992) 80–82.
- [28] B.R. Hacker, L. Ratschbacher, L. Webb, T. Ireland, D. Walker, S. Dong, U/Pb zircon ages constrain the architecture of the ultrahigh-pressure Qinling-Dabie Orogen, China, *Earth Planet. Sci. Lett.* 161 (1998) 215–230.
- [29] K. Ye, B. Cong, D. Ye, The possible subduction of continental material to depths greater than 200 km, *Nature* 407 (2000) 734–736.
- [30] P.N. Dobbs, D.J. Duncan, S. Hu, S.R. Shee, E. Colgan, M.A. Brown, C.B. Smith, H.L. Allsopp, The geology of the Mengyin kimberlites, Shandong, China, in: H.O.A. Meyer, O.H. Leonardos (Eds.), *Fifth International Kimberlite Conference, Vol. 1, Companhia de Pesquisa de Recursos Minerais, Araxa, 1994*, pp. 40–61.
- [31] J.S. Chi, F.X. Lu, *Formation of Primary Diamond in China*, Press of China University of Geosciences, Wuhan, 1996, 355 pp.
- [32] S. Gao, B.-R. Zhang, Z.-M. Jin, H. Kern, T.-C. Luo, Z.-D. Zhao, How mafic is the lower continental crust?, *Earth Planet. Sci. Lett.* 106 (1998) 101–117.
- [33] S. Hu, L. He, J. Wang, Heat flow in the continental area of China: a new data set, *Earth Planet. Sci. Lett.* 179 (2000) 407–419.
- [34] F.R. Boyd, Compositional distinction between oceanic and cratonic lithosphere, *Earth Planet. Sci. Lett.* 96 (1989) 15–26.
- [35] H.S.C. O'Neill, The transition between spinel lherzolite and garnet lherzolite, and its use as a geobarometer, *Contrib. Mineral. Petrol.* 77 (1981) 185–194.
- [36] F.R. Boyd, D.G. Pearson, S.A. Mertzman, Spinel-facies peridotites from the Kaapvaal root, in: J.J. Gurney, J.L. Gurney, M.D. Pascoe, S.H. Richardson (Eds.), *The J.B. Dawson Volume. Proceedings of the VIIth International Kimberlite Conference, Red Roof Design, Cape Town, 1999*, pp. 40–48.
- [37] D. Smith, F.R. Boyd, Compositional heterogeneities in a high-temperature lherzolite nodule and implications for mantle processes, in: P.H. Nixon (Ed.), *Mantle Xenoliths*, John Wiley and Sons, Chichester, 1987, pp. 551–561.

- [38] K.J. Zhang, Trace element and isotope characteristics of Cenozoic basalts around the Tanlu Fault with implications for the Eastern Plate Boundary between North and South China: An extended discussion, *J. Geol.* 108 (2000) 739–743.
- [39] S.-L. Chung, Z.-X. Li, Trace element and isotope characteristics of Cenozoic basalts around the Tanlu Fault with implications for the Eastern Plate Boundary between North and South China: A reply, *J. Geol.* 108 (2000) 743–747.
- [40] M. Faure, W. Lin, N. Le Breton, Where is the North China-South China block boundary in eastern China, *Geology* 29 (2001) 119–122.
- [41] M. Zhai, B. Cong, J. Guo, W. Liu, Y. Li, Q. Wang, Sm-Nd geochronology and petrography of garnet pyroxene granulites in the northern Sulu region of China and their geotectonic implication, *Lithos* 52 (2000) 23–33.
- [42] J.P. Lorand, Are spinel lherzolite xenoliths representative of the abundance of sulfur in the upper mantle?, *Geochim. Cosmochim. Acta* 54 (1990) 1487–1492.
- [43] R.L. Cao, S.-H. Zhu, Mantle xenoliths and alkali-rich host rocks in eastern China, in: P.H. Nixon (Ed.), *Mantle Xenoliths*, John Wiley and Sons, Chichester, 1987, pp. 167–180.
- [44] Y. Song, F.A. Frey, Geochemistry of peridotite xenoliths in basalt from Hannuoba, Eastern China: Implications for subcontinental mantle heterogeneity, *Geochim. Cosmochim. Acta* 53 (1989) 97–113.
- [45] M. Tatsumoto, A.R. Basu, H. Wankang, W. Junwen, X. Guanghong Sr., Nd and Pb isotopes of ultramafic xenoliths in volcanic rocks of Eastern China: enriched components EMI and EMII in subcontinental lithosphere, *Earth Planet. Sci. Lett.* 113 (1992) 107–128.
- [46] S. Chen, S.Y. O'Reilly, X. Zhou, W.L. Griffin, G. Zhang, M. Sun, J. Feng, M. Zhang, Thermal and petrological structure of the lithosphere beneath Hannuoba, Sino-Korean Craton, China: evidence from xenoliths, *Lithos* 56 (2001) 267–301.
- [47] Y.-S. Liu, S. Gao, S.-Y. Jin, S.-H. Hu, M. Sun, Z.-B. Zhao, J.-L. Feng, Geochemistry of lower crustal xenoliths from Neogene Hannuoba Basalt, North China Craton: Implications for petrogenesis and lower crustal composition, *Geochim. Cosmochim. Acta* 65 (2001) 2589–2604.
- [48] J.T. Chesley, R.L. Rudnick, C.-T. Lee, Re-Os systematics of mantle xenoliths from the East African Rift: Age, structure, and history of the Tanzanian craton, *Geochim. Cosmochim. Acta* 63 (1999) 1203–1217.
- [49] R.W. Carlson, D.G. Pearson, F.R. Boyd, S.B. Shirey, G. Irvine, A.H. Menzies, J.J. Gurney, Re-Os systematics of lithospheric peridotites: implications for lithosphere formation and preservation, in: J.J. Gurney, J.L. Gurney, M.D. Pascoe, S.H. Richardson (Eds.), *The J.B. Dawson volume, Proceedings of the VIIth International Kimberlite Conference*, Red Roof Design, Cape Town, 1999, pp. 99–108.
- [50] R.J. Walker, R.W. Carlson, S.B. Shirey, F.R. Boyd, Os, Sr, Nd, and Pb isotope systematics of southern African peridotite xenoliths implications for the chemical evolution of the subcontinental mantle, *Geochim. Cosmochim. Acta* 53 (1989) 1583–1595.
- [51] M.R. Handler, V.C. Bennett, T.M. Esat, The persistence of off-cratonic lithospheric mantle: Os isotopic systematics of variably metasomatised southeast Australian xenoliths, *Earth Planet. Sci. Lett.* 151 (1997) 61–75.
- [52] L. Reisberg, J.-P. Lorand, Longevity of sub-continental mantle lithosphere from osmium isotope systematics in orogenic peridotite massifs, *Nature* 376 (1995) 159–162.
- [53] M.R. Handler, V.C. Bennett, G. Dreibus, Evidence from correlated Ir/Os and Cu/S for late-stage Os mobility in peridotite xenoliths: Implications for Re-Os systematics, *Geology* 27 (1999) 75–78.
- [54] D.J. DePaolo, G.J. Wasserburg, Nd isotopic variation and petrogenetic models, *Geophys. Res. Lett.* 3 (1976) 249–252.
- [55] T. Meisel, R.J. Walker, A.J. Irving, J.-P. Lorand, Osmium isotopic compositions of mantle xenoliths: A global perspective, *Geochim. Cosmochim. Acta* 65 (2001) 1311–1323.
- [56] K.W. Burton, P. Schiano, J.-L. Birck, C.J. Allègre, Osmium isotope disequilibrium between mantle minerals in a spinel-lherzolite, *Earth Planet. Sci. Lett.* 172 (1999) 311–322.
- [57] K.W. Burton, P. Schiano, J.-L. Birck, C.J. Allègre, M. Rehkämper, A.N. Halliday, J.B. Dawson, The distribution and behaviour of rhenium and osmium amongst mantle minerals and the age of the lithospheric mantle beneath Tanzania, *Earth Planet. Sci. Lett.* 183 (2000) 93–106.
- [58] N.J. Pearson, O. Alard, W.J. Griffin, S.Y. O'Reilly, S.E. Jackson, Re-Os isotopes in sulfides in mantle peridotites: a record of melt depletion and metasomatism, in: *Eleventh Annual V.M. Goldschmidt Conference*, Abstract #3316, LPI Contribution No. 1088, Lunar and Planetary Institute, Houston, TX (CD-ROM), 2001.
- [59] O. Alard, W.L. Griffin, J.P. Lorand, S.E. Jackson, S.Y. O'Reilly, Non-chondritic distribution of the highly siderophile elements in mantle sulphides, *Nature* 407 (2000) 891–894.
- [60] W.M. Fan, H.F. Zhang, J. Baker, K.E. Jarvis, P.R.D. Mason, M.A. Menzies, On and off the North China Craton: where is the Archaean keel?, *J. Petrol.* 41 (2000) 933–950.
- [61] C.-T. Lee, Q. Yin, R.L. Rudnick, J.T. Chesley, S.B. Jacobsen, Osmium isotopic evidence for Mesozoic removal of lithospheric mantle beneath the Sierra Nevada, California, *Science* 289 (2000) 1912–1916.
- [62] I.J. Parkinson, C.J. Hawkesworth, A.S. Cohen, Ancient mantle in a modern arc: Osmium isotopes in Izu-Bonin-Mariana forearc peridotites, *Science* 281 (1998) 2011–2013.
- [63] S. Esperança, S.E. Sichel, M.F. Horan, R.J. Walker, T. Juteau, R. Hekinian, Some abyssal peridotites are old!, in: *Ninth Annual V.M. Goldschmidt Conference*, Ab-

- stract #7389, LPI Contribution No. 971, Houston, TX (CD-ROM), 1999.
- [64] M.A. Menzies, Y. Xu, Geodynamics of the north China Craton, in: M. Flower, S.-L. Chung, C.-H. Lo, T.-Y. Lee (Eds.), *Mantle Dynamics and Plate Interactions in East Asia*, American Geophysical Union, Washington, DC, 1998, pp. 155–165.
- [65] W.F. McDonough, S.-s. Sun, Composition of the Earth, *Chem. Geol.* 120 (1995) 223–253.
- [66] A.D. Brandon, J.E. Snow, R.J. Walker, J.W. Morgan, T.D. Mock,  $^{190}\text{Pt}$ - $^{186}\text{Os}$  and  $^{187}\text{Re}$ - $^{187}\text{Os}$  systematics of abyssal peridotites, *Earth Planet. Sci. Lett.* 177 (2001) 319–335.
- [67] K.R. Ludwig, ISOPLOT: A Plotting and Regression Program for Radiogenic-isotope Data, U.S. Geol. Surv. Open-File Rep., 1991, 39 pp.
- [68] J.M. Rhodes, Geochemical stratigraphy of lava flows sampled by the Hawaiian scientific drilling project, *J. Geophys. Res.* 101 (1996) 11,726–11,746.